

Magnetic Band Gap Opening in Long Sequences of Rhombohedral-stacked Multilayer Graphene

Hugo Henck¹, Jose Avila², Zeineb Ben Aziza¹, Debora Pierucci³, Jacopo Baima⁴, Betül Pamuk⁴, Julien Chaste¹, Daniel Utt⁵, Miroslav Bartos⁵, Karol Nogajewski⁵, Benjamin A. Piot⁵, Milan Orlita⁵, Marek Potemski⁵, Matteo Calandra⁴, Maria C. Asensio², Francesco Mauri^{6,7}, Clément Faugeras^{5,*} and Abdelkarim Ouerghi^{1,*}

¹Centre de Nanosciences et de Nanotechnologies, CNRS, Univ. Paris-Sud, Université Paris-Saclay, C2N – Marcoussis, 91460 Marcoussis, France

²Synchrotron-SOLEIL, Saint-Aubin, BP48, F91192 Gif sur Yvette Cedex, France

³CELLS - ALBA Synchrotron Radiation Facility, Carrer de la Llum 2-26, 08290 Cerdanyola del Valles, Barcelona, Spain

⁴Institut de Minéralogie, de Physique des Matériaux, et de Cosmochimie, UMR CNRS 7590, Sorbonne Universités, UPMC, Univ. Paris VI, MNHN, IRD, 4 Place Jussieu, 75005 Paris, France

⁵Laboratoire National des Champs Magnétiques Intenses, CNRS-UGA-UPS-INSA-EMFL, 25 rue des Martyrs, 38042 Grenoble, France

⁶Departimento di Fisica, Università di Roma La Sapienza, Piazzale Aldo Moro 5, I-00185 Roma, Italy

⁷Graphene Laboratories, Fondazione Istituto Italiano di Tecnologia, 16163 Genova, Italy

*Corresponding authors, E-mail: abdelkarim.ouerghi@c2n.upsaclay.fr

E-mail: clement.faugeras@lncmi.cnrs.fr

ABSTRACT

Attempts to induce a clean and stabilized gap in the excitation spectrum of graphene,¹⁻³ or a robust magnetism⁴⁻⁶ preserving a high carrier mobility have not been successful yet. An alternative procedure to achieve an optical gap and a magnetic state in graphene is to explore correlated states in flat electronic bands hosted by multilayer graphene with rhombohedral stacking⁷⁻⁹. The low kinetic energy of such carriers could lead to gap opening even at weak Coulomb repulsion by stabilizing a magnetic or superconducting state. Here, we directly image the band structure of large graphitic flake containing approximately 14 consecutive ABC layers. We reveal the flat electronic bands and identify a gapped magnetic state by comparing angle-resolved photoemission spectroscopy with first-principle calculations. The gap is robust and stable at liquid nitrogen temperature. Our work opens up new perspectives in the development of optoelectronic and spintronic devices made of easily processable carbon materials.

KEYWORDS: Flat Band - Band Gap - Rhombohedral Multilayer Graphene - Density Functional Theory - Angle-resolved Photoemission Spectroscopy

Introduction:

Spintronic applications require surface magnetic states that are difficult to stabilize in weakly correlated carbon based materials. The attempt to stabilize magnetism in these systems is highly desirable as it could lead to easily processable, environmentally friendly and economically attractive devices. Due to lack of a band gap the application of graphene in optoelectronic devices is severely limited as its electrical conduction cannot be switched off using control voltages. In graphene, the delocalized nature of π orbitals leads to a high Fermi velocity and to a large kinetic energy of Dirac electrons, hindering the stabilization of a magnetic state with a sizeable gap. For this reason, bandgap engineering in graphene has mostly focused so far on different procedures that do not involve electronic correlation, such as nanolithography of nanoribbon and dots¹⁻³, field-induced band-gap opening¹⁰ or chemical functionalization.¹¹ Recently, however, several theoretical calculations⁷⁻⁹ predicted the occurrence of an ultraflat surface state (bandwidth smaller than 2 meV) at the K and K' corners of the Brillouin zone in the outer layers of multilayer graphene with rhombohedral stacking (ABC). A drastic reduction of kinetic energy associated with this state makes it possible, in principle, to obtain correlated bandgap opening and stabilization of magnetic, superconducting or charge density wave states, even under moderate electron repulsion. Thus, electrons' correlation in the surface state of ABC multilayer graphene is a new pathway towards gap engineering in graphene.

The largest difficulty in pursuing this route is the isolation of multilayer graphene with long ABC sequences mainly because rhombohedral graphite is less stable in ambient conditions, and hence less abundant^{12,13} than Bernal graphite (ABA). With all the recent efforts to (re)visit the electronic properties of bulk and thin films graphite, the ABC stacked graphene trilayer has been successfully identified and studied experimentally^{14,15}. It shows many remarkable properties such as a band gap at charge neutrality conditions with a magnitude tunable by applying an electric field^{16,17} and it also hosts chiral massive Dirac fermions as evidenced by their peculiar Quantum Hall Effect^{16,18}. Furthermore, transport measurements on suspended ABC trilayers display an opening of a 40 meV gap, tentatively attributed to a magnetic state¹⁹. However, this magnetic state is fragile as it occurs only in ultra-clean samples and is destroyed by temperature ($T_c = 30 - 40$ K) or by the presence of a substrate²⁰.

Increasing the number of ABC-stacked layers is important as the extent in k-space of the flat band-energy dispersion is developing. Furthermore, with the increase of electronic correlation in the flat-band, the electronic ground state in long ABC sequences band has been predicted to

be superconducting^{7,8,21} or magnetic²². Experiments on mixtures of ABA- and ABC- stacked graphite are interpreted in terms of superconductivity²³ but there exist up to now no experiments addressing single crystals with a large ABC stacked sequence mainly due to the lack of established ABC-stacked graphite source. A larger sequence of 15 ABC-stacked graphene layers has recently been produced by exfoliation, and its Landau level fan chart was determined by magneto-Raman scattering²⁴. A proper and systematic investigation of the electronic properties of ABC stacked graphite is still lacking. Here, we study for the first time the band structure of a large sequence of ABC-stacked graphene multilayer by using angle-resolved photoemission spectroscopy (ARPES). We show that it is possible to isolate flakes with about 14 consecutive layers with rhombohedral staking and with a lateral size up to 20 x 80 micrometres. Our ARPES results demonstrate the presence of a band gap in ABC graphene multilayer. Its band structure is compared to the one of a Bernal-stacked domain of similar thickness. Such a band gap is not observable in ABA graphene multilayer in the same conditions. Ab initio calculations allow to identify this gap as originating from the exchange interaction among electrons in the flat surface states. The signature of the magnetic state is evident at liquid nitrogen temperature and in supported samples. The electronic ground state is hence spin polarized which means that thin layers of rhombohedral graphite can offer an interesting platform for optoelectronics and spintronics applications.

Results and discussions:

Graphene multilayers exhibit two structures with Bernal (Figure 1(a)) and rhombohedral (Figure 1(b)) stacking (ABA and ABC respectively). Our thin rhombohedral graphite layer was produced by mechanical exfoliation of Kish graphite on a polydimethylsiloxane (PDMS) stamp. Flakes with ABC stacking were then identified based on their Raman scattering response²⁴ and, in particular, on the line shape of the 2D band feature. Because the 2D band feature arises from a double resonant Raman scattering process, it directly involves the electronic band structure and is hence a sensitive probe of the stacking configuration²⁵. The 2D band in ABC stacked multilayer graphene appears as a multi-component feature which is significantly broader than the one in ABA stacked thin graphite, and, for a given thickness, this criterion is sufficient to discriminate between the two stacking configurations (Figure 1(c) and (d)). Clearly two domains are present in the flake: one with ABA stacking and the other with ABC stacking. The ABC part has a large spatial extension with size up to 20 x 80 micrometres (Figure 1(e)). More details on Raman scattering characterization of our sample

are provided in the Supplementary information (SI). The selected flake was then deterministically transferred onto a graphitized 4H-SiC substrate, with a conductive graphene monolayer (1 ML Gr) at the surface, which is particularly well adapted for ARPES measurements²⁶. The graphene used was obtained by annealing 4H-SiC(0001) at 1550 °C in 800 mbar argon for 10 min^{27,28}. Figure 1(f) shows an optical micrograph of a graphene multilayer flake after its transfer to the graphitized 4H-SiC. Typical AFM images of the sample are reported in Figure S1(a). The different profile scan presented in Figure S1(b) allowed us to measure the height of the flake and we obtained an estimation of the layers number of about 50 – 60 Layers.

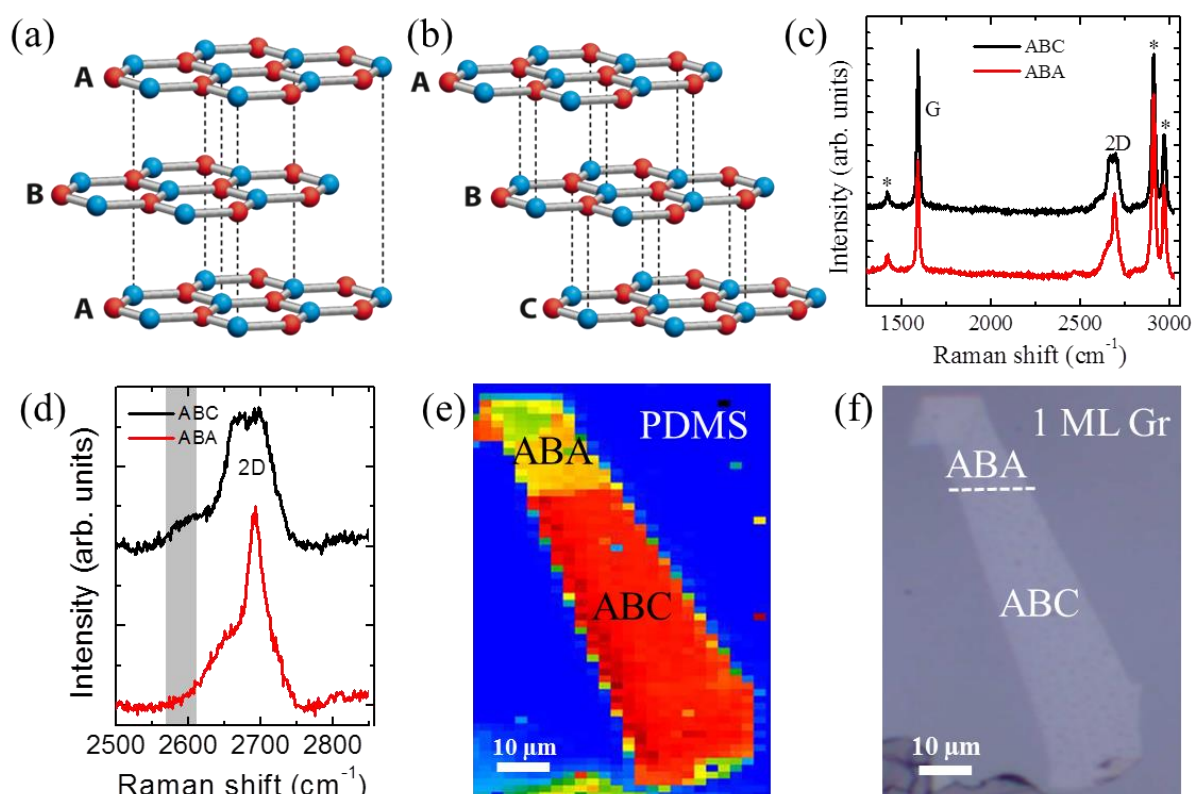


Figure 1 (Color online): Schematic representation of multilayer graphene structure and their Raman signature: Top view of (a) ABA and (b) ABC stacking sequences of multilayer graphene. The colored layers differentiate the successive position in the in-plane direction where each color corresponds to an inequivalent layer position. (c) Raman scattering spectra of ABC- (black curve) and ABA- (red curve) stacked thin graphite measured on a flake on polydimethylsiloxane (PDMS) stamp. The G band and 2D bands are indicated and the star symbols indicate Raman scattering features from PDMS. (d) Zoom of ABC- (black curve) and ABA- (red curve) stacked graphene 2D peak. (e) False color spatial map of the integrated intensity in the shaded energy range in Figure 1(d), where a significant difference is observed

between ABC and ABA, (f) Optical image of the studied flake.

To resolve the electronic structure of graphene multilayer described above, we have performed nano-ARPES measurements at synchrotron Soleil at liquid nitrogen temperature (90 K), with a spatial resolution of 100 nm. Due to the transfer process, the BZ of graphene multilayer is rotated by 17° with respect to the graphene BZ (Figure 2(a)). In Figure 2(b) we show the averaged ARPES map coming from the multilayer graphene flake shown in Figure 1(f). The photoemission intensity around the K-point for the graphene multilayer was acquired along the Γ KM direction for a photon energy $h\nu = 100$ eV as a function of space coordinate. The ARPES intensity was then integrated over different energy ranges illustrated by the three colored rectangles A, B and C in Figure 2(b). Figure 2(c) shows a spatially resolved map integrated from 1 eV to the Fermi energy E_F (green rectangle) and demonstrates the homogeneity of the ARPES intensity over the flake, thus confirming its uniform thickness. Figure 2(d) and (e) show spatially-resolved maps integrated from 150 meV to 250 meV and from 100 meV to E_F , respectively (red and yellow rectangles respectively). Different regions on the flakes can be identified based on these integrated intensity maps. The large background region with low ARPES intensity (outside the white dotted line) represents the band structure of the monolayer graphene/SiC substrate as labeled with 1ML Gr in Figure 1(f). As can be seen by the different ARPES intensities, the flake is composed of two areas of size in the μm range. In agreement with the micro-Raman measurement (Figure 1(d)), these two areas correspond to an ABA (Figure 2(d)) and ABC (Figure 2(e)) stacked multilayer graphene. The fact that ABA and ABC stacking presents a different ARPES intensity in different energy ranges is strictly related to their different electronic structure as shown in Figure 3.

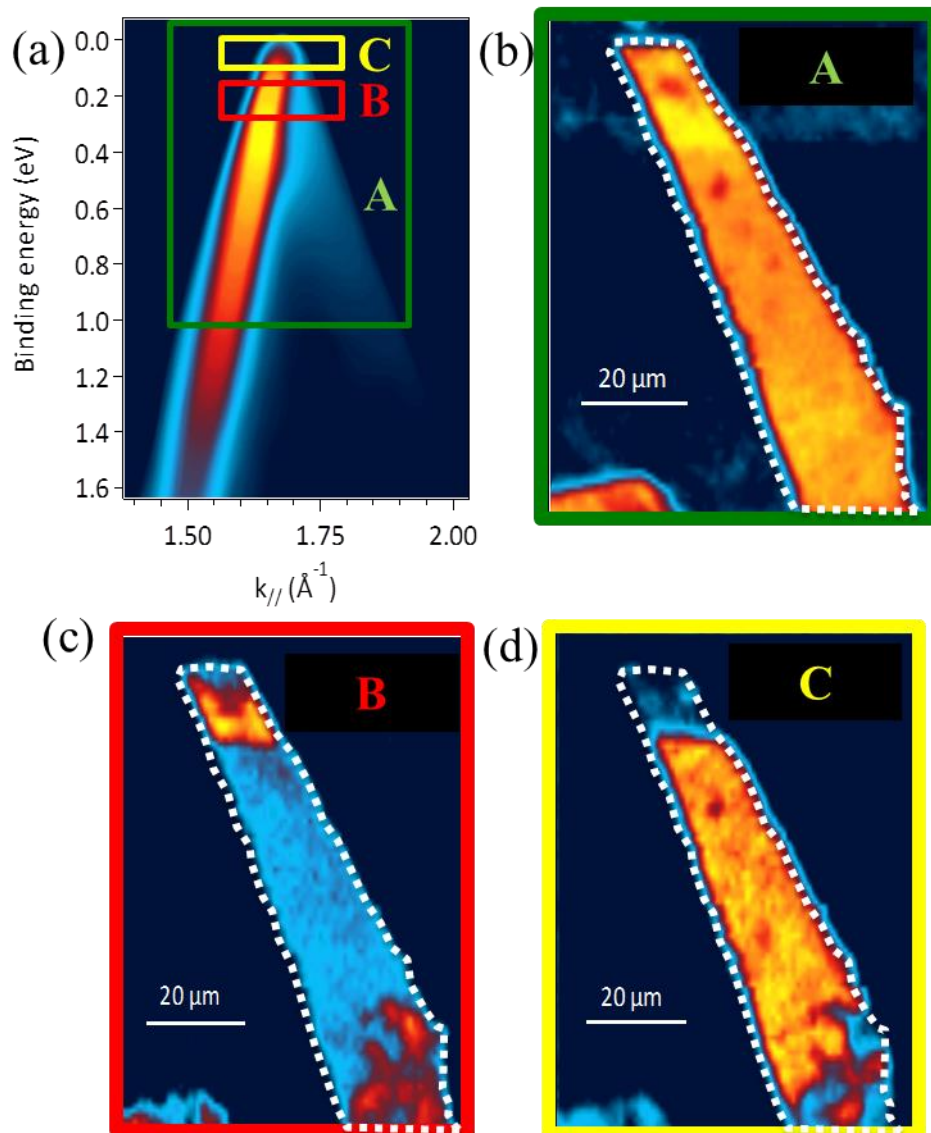


Figure 2 (Color online): Spatially-resolved electronic structure of an exfoliated graphene multilayer flake: (a) Typical Nano-ARPES intensity map of an ABA stacked graphene. (b-d) Spatial false color map built from nanoARPES intensity map of an exfoliated graphene multilayer structure transferred onto graphene-SiC(0001) substrate showing the ABC and ABA stacked inclusion. The colored rectangles in (a) indicate the energy integration range where the spatially resolved maps of (b-d) have been recorded.

Figure 3(a-c) show nano-ARPES intensity maps measured at three different locations: 1ML Gr, ABA and ABC that were identified by ARPES and micro-Raman scattering (see Figure

1(d) and Figure 2). The observed electronic band structures for the ABA and ABC areas are very different despite the similar thickness of the flake at these locations. Detailed dispersions of different π bands in the vicinity of the K and K' special points are well resolved. The linear dispersion of single layer graphene of the substrate under the flake is very clear in Figure 3(a). Figure 3(b) shows the band structure at the ABA location, where different bands can be observed. The main two bands have a quadratic dispersion, are split by ~ 200 meV and are identified as the two split-off bands at the K point of the ABA graphene multilayer²⁹. The ARPES response measured over the ABC domain is completely different (Figure 3(c)). It consists of an intense band close to E_F with a flat dispersion, and two cone-like structures composed of a manifold of bands (Figure 3(d)). The flat band at the Fermi level is also confirmed by the energy distribution curves (EDC) at the K point with a 25 meV bandwidth (Figure 3(e)). This picture precisely reflects the expected band structure of rhombohedral graphene multilayer⁹.

From these results we can clearly confirm that the sample is composed of a small domain with Bernal stacking and a larger domain with a broad ABC-stacked sequence of graphene layers, in accordance with Raman spectroscopy and a flat dispersion of the surface state. The measured ARPES band structure is thus consistent with the occurrence of a long rhombohedral sequence and the undoped surface state. Following the maximum intensity in this map at energies well below the Fermi level, a linear-shaped dispersion is observed. One can also note that this sample appears to be quasi neutral, with the Fermi energy close to the charge neutrality point. This observation, is supported by the the energy distribution curves (EDC) of the K point of the band structure (Figure 3(e)).

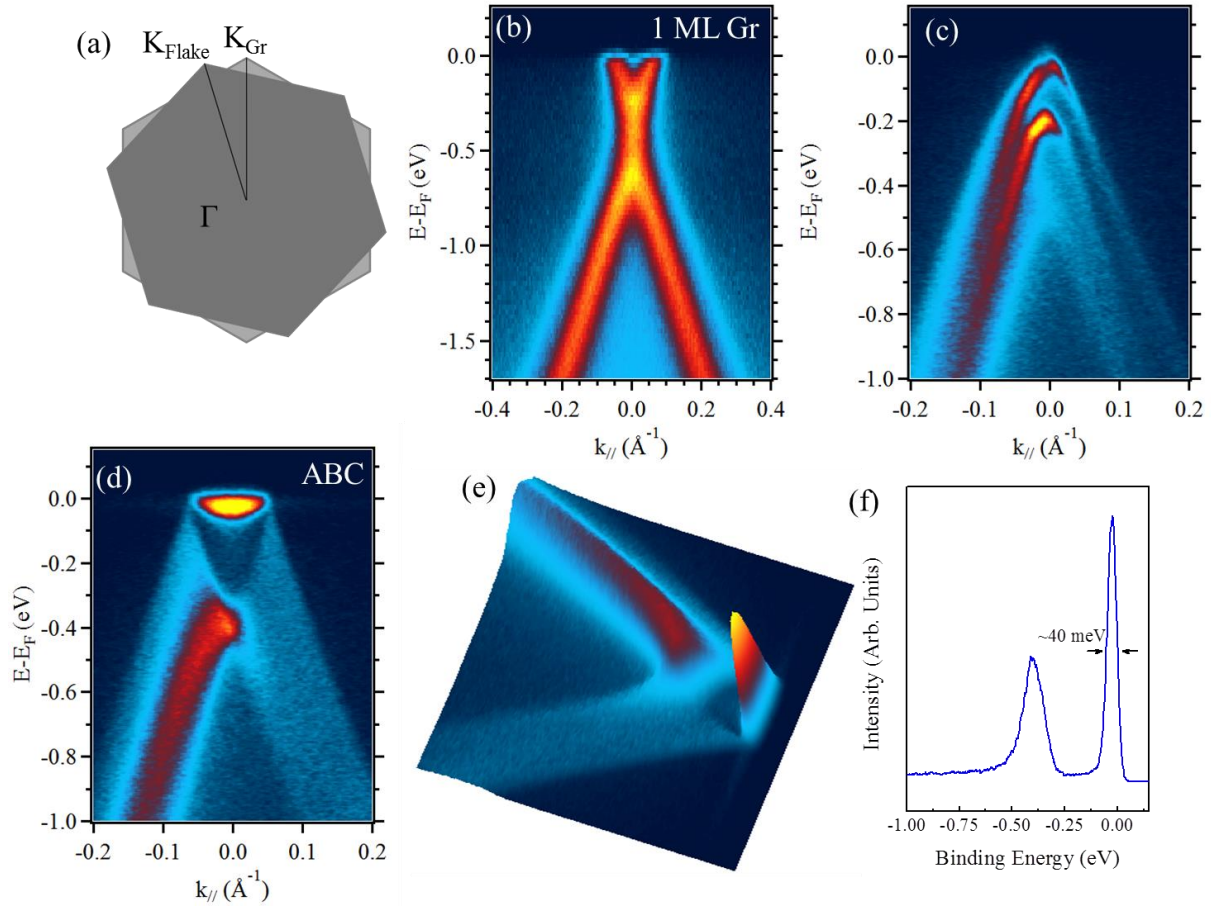


Figure 3 (Color online): **Angle-resolved electronic structure of an exfoliated graphene multilayer:** **a)** Brillouin zone of graphene and graphene multilayer flake with a twist angle of 17° , ARPES intensity maps around the K point of the Brillouin zone for **(b)** the monolayer graphene substrate, recorded in the direction perpendicular to ΓK , **(c)** ABA and **(d)** ABC regions of the flake recorded along the ΓKM direction. The spectra were measured with photon energy of 100 eV. **(e)** 3D plot of the ARPES intensity map for the ABC region shown in **(d)**. **(f)** ARPES intensity spectra of ABC-stacked graphene multilayer at the K point of the graphene Brillouin zone.

A more detailed inspection of the electronic band dispersion close to E_F at the ABC location shows that it is not exactly flat, in fact a curvature in the ΓK and KM directions is present. From the analysis of the energy distribution curves (EDC) shown in [Figure 4\(a\)](#), we conclude that higher density of surface states occurs at the Fermi level. We underline that the dispersion of the surfaces states band is about 25 meV and the flattening of the band top still amounts to 0.13 \AA^{-1} near the K points. This can be particularly appreciated in the second derivative of ARPES response with respect to energy shown in [Figure 4\(b\) and \(c\)](#). The flat band near the

K point extends by about 0.13 \AA^{-1} , disperses in the Γ K and KM directions towards the valence band maximum, and extends over 25 meV. The flat band extension in k-space is strictly related to the length of the ABC-stacked sequence corresponding, in our case, to 14 ABC-stacked graphene layers. This value is different with the AFM measurement. This difference can be attributed to a stacking fault (twisted angle of about $2^\circ/3^\circ$) between the topmost and bottom layers is present, thus decoupling the 14 rhombohedral stacking layers from the bottom²⁰.

To gain further insight into the electronic structure of ABC graphite, we performed first-principles electronic structure calculations with inclusion of an exact exchange (see SI). We considered a 14-layer crystal with the ABC stacking and we included a 37 \AA vacuum gap between the periodic images. We performed spin-polarized and unpolarized calculations. The same rescaling of the Fermi velocity found for graphene was applied. By neglecting spin polarization, the electronic structure displays an extremely narrow metallic surface state (bandwidth smaller than 2 meV) localized around the K-point in the Brillouin zone. This is in disagreement with the experiment, which established a substantially larger bandwidth (25 meV). The two cones formed by an ensemble of electronic bands corresponding to the bulk states, and intersecting at the K point at an energy of - 400 meV are well reproduced. By introducing the spin polarization, an antiferromagnetic state is stabilized, in agreement with the findings of Ref 9 obtained, however, for thinner flakes. The largest magnetic moments are on the outer layers and they gradually decrease towards the center of the flakes. The coupling between the layers is antiferromagnetic, while the coupling inside the layers is slightly ferrimagnetic. The magnetism does not affect the bulk states electronic structure but it results in an insulating surface state with a gap opening of 40 meV. Our calculations show that this band gap originates from the exchange interaction which lifts the spin degeneracy of the flat band states. Interestingly, the effective mass of the top of the valence band (surface state) is now in perfect agreement with the 25 meV dispersion found in ARPES experiments (see [Figure 4 \(b\) and \(c\)](#)).

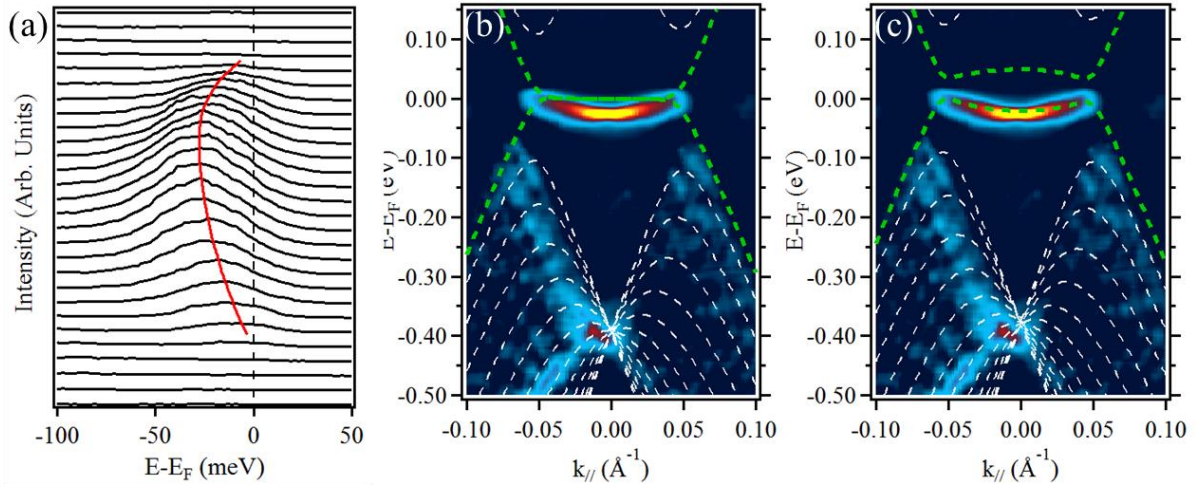


Figure 4 (Color online): Energy vs momentum dispersion relation of ABC-stacked graphene multilayer's flat band: (a) ARPES energy distribution curves of 14-layer sequence of ABC-stacked graphene multilayer showing the presence of a flat band around the charge neutrality point. The red line was obtained by fitting the maximum intensity of the curves with a parabolic dispersion. (b) and (c) Second derivative of ABC graphene ARPES intensity map compared with theoretical calculation of 14-layer sequence of graphite (b) without and (c) with the spin polarization. White dashed curves in these graphs correspond to bulk states and green dashed curves highlight the surface state of the outer layers.

The extension of the flat surface state in the Brillouin zone (0.13 \AA^{-1}) is also well reproduced. The good agreement between theory and experiments strongly supports the presence of a gapped magnetic state in ABC multilayers. Remarkably, while a Curie temperature of 34 K was determined from transport measurements done on ABC trilayers¹⁹, here, in our thicker flake, we find that magnetism survives up to at least liquid nitrogen temperature. In summary, we have successfully isolated a large graphene multilayer flake with a long sequence of ABC stacking. By performing high-resolution nano-ARPES experiments, we have spatially mapped its electronic band structure. By comparing nano-ARPES results and first-principles electronic structure calculations we have shown that a gap opening compatible with a magnetic state occurs in such a system at liquid nitrogen temperature. The exchange interaction lifts the spin degeneracy of the flat band and opens an energy gap of $\sim 40 \text{ meV}$. The magnetic gap is robust as it occurs in a supported sample and its Curie temperature is at least 90 K, much larger than what found in suspended ABC trilayers. Our work opens up a new route towards band gap engineering in graphene-based materials, namely the exploitation of the electron-electron interaction in the surface bands of long sequences ABC-stacked graphene multilayers. In the

future, the capability of developing ABC sequences of desired length and of controlling the stacking order in graphene multilayers could lead to optoelectronic devices with tunable optical properties. Furthermore, the stabilization of an intrinsic magnetic gap in a carbon based material and the occurrence of spin-polarized magnetic surface states is a major step towards graphene spintronic.

Acknowledgements: This work was supported by the ANR H2DH grant, by the European Research Council (MOMB project no. 320590) and by the EC Graphene Flagship project (no. 604391). We acknowledge the support from the European Union Horizon 2020 research and innovation program under Grant agreement No. 696656-GrapheneCore1. B. P. acknowledges the support from the National Science Foundation (Platform for the Accelerated Realization, Analysis, and Discovery of Interface Materials (PARADIM)) under Cooperative Agreement No. DMR-1539918. Computer facilities were provided by CINES, IDRIS, and CEA TGCC (Grant EDARI No. 2017091202).

REFERENCES

1. Han, M. Y., Ozyilmaz, B., Zhang, Y. & Kim, P. Energy band-gap engineering of graphene nanoribbons. *Phys. Rev. Lett.* **98**, 206805 (2007).
2. Li, X., Wang, X., Zhang, L., Lee, S. & Dai, H. Chemically Derived, Ultrasoft Graphene Nanoribbon Semiconductors. *Science (80-.)*. **319**, 1229–1232 (2008).
3. Ponomarenko, L. A. *et al.* Chaotic Dirac billiard in graphene quantum dots. *Science (80-.)*. **320**, 356–358 (2008).
4. Krasheninnikov, A. V., Lehtinen, P. O., Foster, A. S., Pyykkö, P. & Nieminen, R. M. Embedding transition-metal atoms in graphene: Structure, bonding, and magnetism. *Phys. Rev. Lett.* **102**, 126807 (2009).
5. Boukhvalov, D. W., Katsnelson, M. I. & Lichtenstein, A. I. Hydrogen on graphene: Electronic structure, total energy, structural distortions and magnetism from first-principles calculations. *Phys. Rev. B - Condens. Matter Mater. Phys.* **77**, (2008).
6. Yazyev, O. V. & Helm, L. Defect-induced magnetism in graphene. *Phys. Rev. B - Condens. Matter Mater. Phys.* **75**, 125408 (2007).
7. Kopnin, N., Ijäs, M., Harju, A. & Heikkilä, T. High-temperature surface superconductivity in rhombohedral graphite. *Phys. Rev. B* **87**, 140503(R) (2013).
8. Kopnin, N. B., Heikkilä, T. T. & Volovik, G. E. High-temperature surface superconductivity in topological flat-band systems. *Phys. Rev. B* **83**, 220503 (2011).
9. Baima, J., Mauri, F. & Calandra, M. Magnetic gap opening in rhombohedral-stacked

- multilayer graphene from first principles. *Phys. Rev. B* **75**422, (2017).
10. Oostinga, J. B., Heersche, H. B., Liu, X., Morpurgo, A. F. & Vandersypen, L. M. K. Gate-induced insulating state in bilayer graphene devices. *Nat. Mater.* **7**, 151–157 (2008).
 11. Luo, Z., Vora, P., Mele, E. J., Jr, A. T. C. J. & Kikkawa, J. M. Photoluminescence and Band Gap Modulation in Graphene Oxide Photoluminescence and Band Gap Modulation in Graphene Oxide. *Appl. Phys. Lett.* **94**, 111909 (2009).
 12. Yuan, S., Roldán, R. & Katsnelson, M. I. Landau level spectrum of ABA- and ABC-stacked trilayer graphene. *Phys. Rev. B* **84**, 125455 (2011).
 13. Norimatsu, W. & Kusunoki, M. Selective formation of ABC-stacked graphene layers on SiC(0001). *Phys. Rev. B* **81**, 161410(R) (2010).
 14. Bao, W. *et al.* Stacking-dependent band gap and quantum transport in trilayer graphene. *Nat. Phys.* **7**, 948–952 (2011).
 15. Zhang, W. *et al.* Molecular adsorption induces the transformation of rhombohedral- to Bernal-stacking order in trilayer graphene. *Nat. Commun.* **4**, 2074 (2013).
 16. Zou, K., Zhang, F., Clapp, C., MacDonald, a H. & Zhu, J. Transport studies of dual-gated ABC and ABA trilayer graphene: band gap opening and band structure tuning in very large perpendicular electric fields. *Nano Lett.* **13**, 369–73 (2013).
 17. Hui, Y. Y., Liu, X., Jie, W., Chan, N. Y., Hao, J., Hsu, Y. T., Li, L. J., Guo W., Lau, S. P. Exceptional Tunability of Band Energy in a Compressively Strained Trilayer. *ACS Nano* **7**, 7126–7131 (2013).
 18. Lui, C. H., Li, Z., Mak, K. F., Cappelluti, E. & Heinz, T. F. Observation of an electrically tunable band gap in trilayer graphene. *Nat. Phys.* **7**, 944–947 (2011).
 19. Lee, Y. *et al.* Competition between spontaneous symmetry breaking and single-particle gaps in trilayer graphene. *Nat. Commun.* **5**, 5656 (2014).
 20. Pierucci, D. *et al.* Evidence for Flat Bands near the Fermi Level in Epitaxial Rhombohedral Multilayer Graphene. *ACS Nano* 5432–5439 (2015).
 21. Beth, C. E. P. and P. D. E. and A. C. and J. B.-Q. and M. Z. and S. M.-L. and A. S. and W. B. and D. S. and J. M. and T. M. and O. B. and G. K. an. Identification of a possible superconducting transition above room temperature in natural graphite crystals. *New J. Phys.* **18**, 113041 (2016).
 22. Olsen, R., van Gelderen, R. & Smith, C. Ferromagnetism in ABC-stacked trilayer graphene. *Phys. Rev. B* **87**, 115414 (2013).
 23. Zoraghi, M. *et al.* Influence of rhombohedral stacking order in the electrical resistance of bulk and mesoscopic graphite. *Phys. Rev. B* **95**, 45308 (2017).
 24. Henni, Y. *et al.* Rhombohedral multilayer graphene: A magneto-Raman scattering study. *Nano Lett.* **16**, 3710–3716 (2016).
 25. Torche, A., Mauri, F., Charlier, J.-C. & Calandra, M. The Raman fingerprint of rhombohedral graphite. *arXiv* (2017). at <<http://arxiv.org/abs/1706.02773>>

26. Henck, H. *et al.* Direct observation of the band structure in bulk hexagonal boron nitride. *Phys. Rev. B* **95**, 85410 (2017).
27. Lalmi, B. *et al.* Flower-shaped domains and wrinkles in trilayer epitaxial graphene on silicon carbide. *Sci. Rep.* **4**, 4066 (2014).
28. Pierucci, D. *et al.* Self-organized metal-semiconductor epitaxial graphene layer on off-axis 4H-SiC(0001). *Nano Res.* **8**, 1026–1037 (2015).
29. Coletti, C. *et al.* Revealing the electronic band structure of trilayer graphene on SiC: An angle-resolved photoemission study. *Phys. Rev. B* **88**, 155439 (2013).

Supplementary Information

Magnetic Band Gap Opening in Long Sequences of Rhombohedral-stacked Multilayer Graphene

Hugo Henck¹, Jose Avila², Zeineb Ben Aziza¹, Debora Pierucci³, Jacopo Baima⁴, Betül Pamuk⁴, Julien Chaste¹, Daniel Utt⁵, Miroslav Bartos⁵, Karol Nogajewski⁵, Benjamin A. Piot⁵, Milan Orlita⁵, Marek Potemski⁵, Matteo Calandra⁴, Maria C. Asensio², Francesco Mauri^{6,7}, Clément Faugeras^{5,*} and Abdelkarim Ouerghi^{1,*}

¹Centre de Nanosciences et de Nanotechnologies, CNRS, Univ. Paris-Sud, Université Paris-Saclay, C2N – Marcoussis, 91460 Marcoussis, France

²Synchrotron-SOLEIL, Saint-Aubin, BP48, F91192 Gif sur Yvette Cedex, France

³CELLS - ALBA Synchrotron Radiation Facility, Carrer de la Llum 2-26, 08290 Cerdanyola del Valles, Barcelona, Spain

⁴Institut de Minéralogie, de Physique des Matériaux, et de Cosmochimie, UMR CNRS 7590, Sorbonne Universités, UPMC, Univ. Paris VI, MNHN, IRD, 4 Place Jussieu, 75005 Paris, France

⁵Laboratoire National des Champs Magnétiques Intenses, CNRS-UGA-UPS-INSA-EMFL, 25 rue des Martyrs, 38042 Grenoble, France

⁶Departimento di Fisica, Università di Roma La Sapienza, Piazzale Aldo Moro 5, I-00185 Roma, Italy

⁷Graphene Laboratories, Fondazione Istituto Italiano di Tecnologia, 16163 Genova, Italy

Methods: The 4H-SiC(0001) substrate was etched with hydrogen (100% H₂) at 1550°C for 10 min. Subsequently, the substrate was annealed at 1000°C under 10⁻⁶ mbar of argon and then at 1550°C under 800 mbar of argon for 10 min¹. To produce thin rhombohedral graphite layers, we have exfoliated Kish graphite onto a PDMS stamp. The flakes of interest were then deterministically transferred onto a graphitized 4H-SiC substrate, suitable for ARPES measurements. The quality of the multilayer graphene transferred onto the graphene underlayer was proved by atomic force microscopy (AFM) and Raman spectroscopy measurements.

ARPES measurement: The sample was annealed at 800 °C to clean the surface before the ARPES measurements. Nano-ARPES experiments were performed on the ANTARES beamline (SOLEIL French synchrotron facility). The ARPES data were taken at photon energy of 100 eV with Scienta R4000 analyzer, using linearly polarized light at a base pressure of 5×10^{-11} mbar. The sample was kept at 90 K during the ARPES measurement. The sample orientation was set as to explore the k-space region around the K point in the Γ KM direction of the Brillouin zone.

First-principle electronic structure calculations: We used the PBE0 functional as implemented in the CRYSTAL code² and a triple- ζ -polarized Gaussian-type basis set³. All technical details are the same as in. Ref. ⁴. We first performed PBE0 calculations on graphene and determined that a 16% reduction of the Fermi velocity is needed to match the experimental electronic structure.⁵

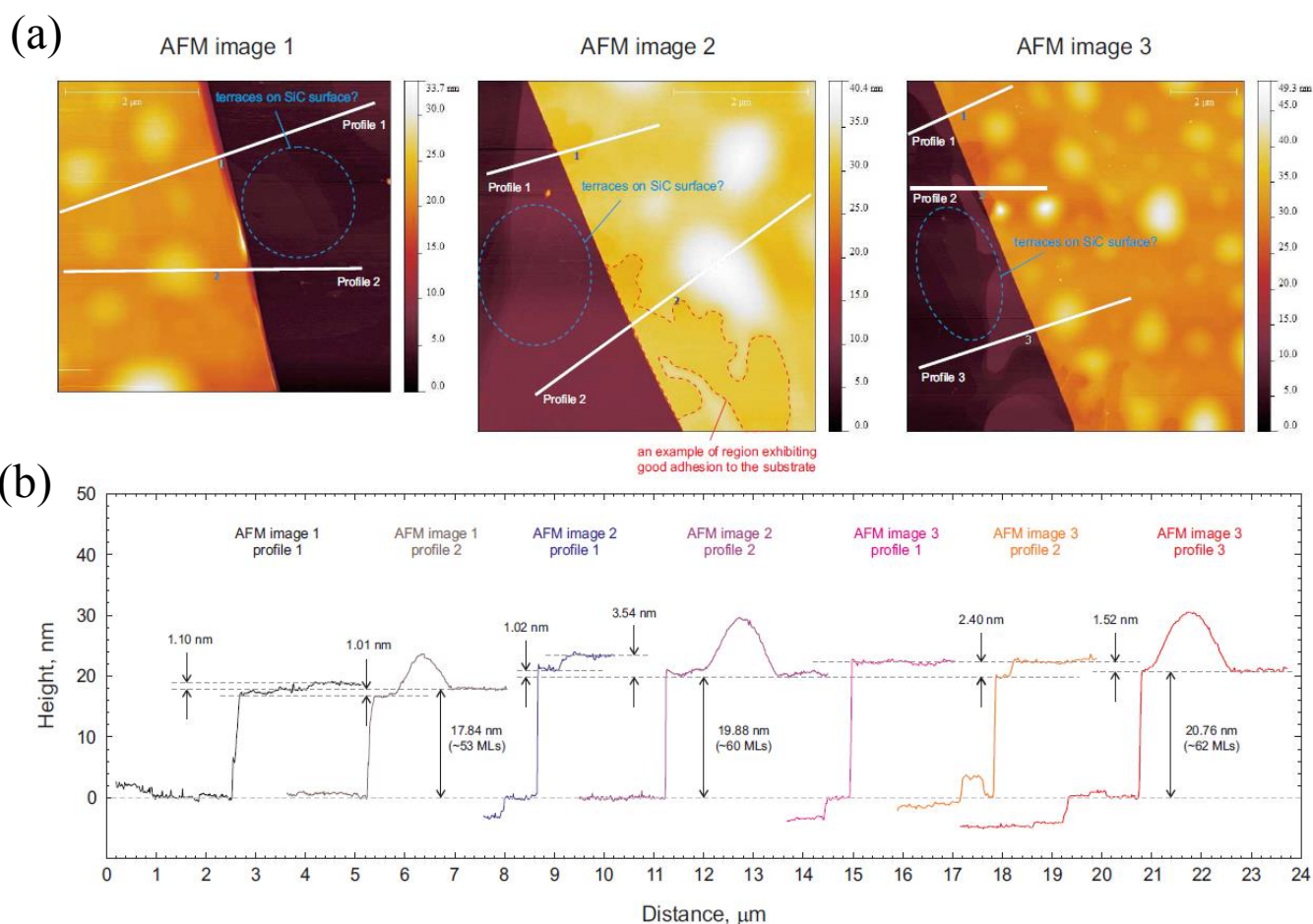


Figure S1: AFM images of ABC stacking graphene multilayer: a) AFM image of graphene multilayer on epitaxial graphene, b) different AFM height profiles corresponding to the line in (a).

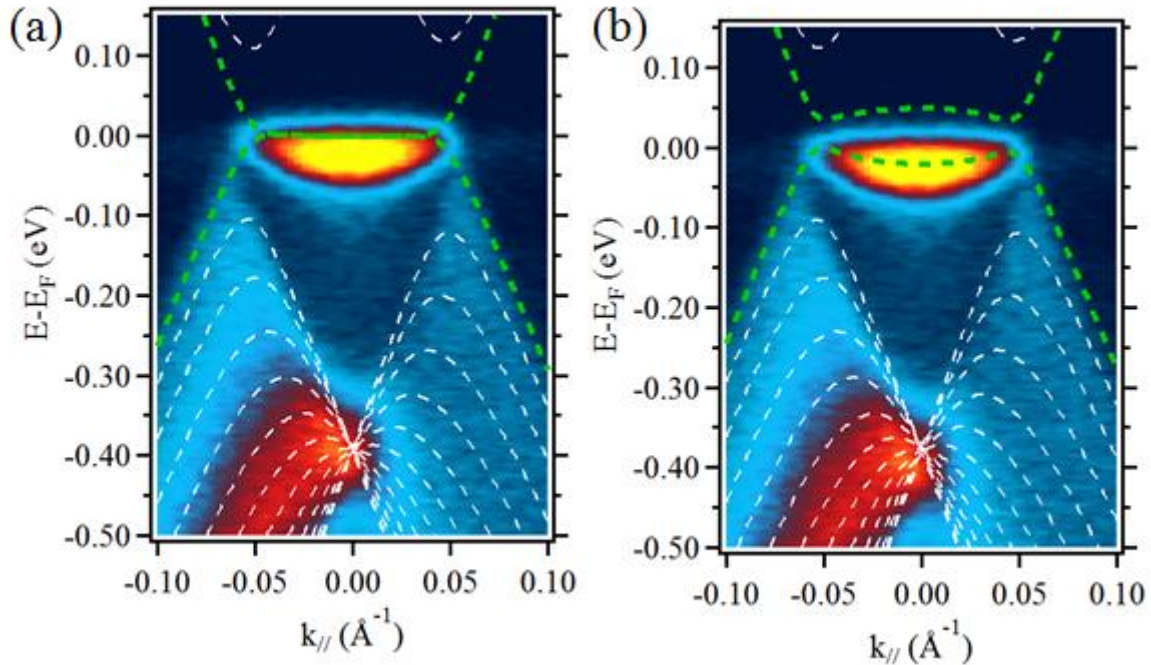


Figure S2: Energy vs momentum dispersion relation of ABC-stacked graphene multilayer's flat band: (a) and (b) ARPES intensity map of ABC graphene compared with theoretical calculation of 14-layer sequence of graphite (b) without and (c) with the spin polarization. White dashed curves in these graphs correspond to bulk states and green dashed curves highlight the surface state of the outer layers.

REFERENCES

1. Pallecchi, E. *et al.* High Electron Mobility in Epitaxial Graphene on 4H-SiC(0001) via post-growth annealing under hydrogen. *Sci. Rep.* **4**, 4558 (2014).
2. Dovesi, R. *et al.* CRYSTAL14 : A program for the ab initio investigation of crystalline solids C RYSTAL 14 : A Program for the Ab Initio Investigation of Crystalline Solids. *Int. J. Quantum Chem.* **34**, (2013).
3. Peintinger, M. F., Oliveira, D. V. & Bredow, T. Consistent Gaussian basis sets of triple-zeta valence with polarization quality for solid-state calculations. *J. Comput. Chem.* **34**, 451–459 (2013).

4. Pamuk, B., Baima, J., Mauri, F. & Calandra, M. Magnetic gap opening in rhombohedral-stacked multilayer graphene from first principles. *Phys. Rev. B* **75422**, (2017).
5. Zhou, S. Y. *et al.* First direct observation of Dirac fermions in graphite. *Nat. Phys.* **2**, 595–599 (2006).